HHS Public Access

Author manuscript

Gynecol Oncol. Author manuscript; available in PMC 2016 August 01.

Published in final edited form as:

Gynecol Oncol. 2015 August ; 138(2): 372–377. doi:10.1016/j.ygyno.2015.05.040.

In vivo tumor growth of high-grade serous ovarian cancer cell lines

Anirban Mitra[1,*], **David A. Davis**[2], **Sunil Tomar**[1], **Lynn Roy**[3], **Hilal Gurler**[4], **Jia Xie**[4], **Daniel D. Lantvit**[2], **Horacio Cardenas**[5], **Fang Fang**[1], **Yueying Liu**[6], **Elizabeth Loughran**[6], **Jing Yang**[6], **M. Sharon Stack**[6,*], **Robert E Emerson**[7,*], **Karen D. Cowden Dahl**[8,*], **Maria Barbolina**[4,*], **Kenneth P. Nephew**[9,*], **Daniela Matei**[5,*], and **Joanna E. Burdette**[2,*]

[1]Medical Sciences Program, Indiana University School of Medicine, Indiana University, Bloomington, IN, United States

[2]Department of Medicinal Chemistry and Pharmacognosy, University of Illinois at Chicago, Chicago, IL, United States

[3]Department of Biochemistry and Molecular Biology, Indiana University School of Medicine-South Bend; Harper Cancer Research Institute, Notre Dame, IN

[4]Department of Biopharmaceutical Sciences, University of Illinois at Chicago, Chicago, IL, United States

[5]Department of Medicine, Indiana University School of Medicine, Indianapolis, IN, United States

[6]Harper Cancer Research Institute, Notre Dame, IN; Department of Chemistry and Biochemistry, University of Notre Dame, Notre Dame, IN, United States

[7]Department of Pathology Indiana University School of Medicine, Indianapolis, IN, United States

[8]Department of Biochemistry and Molecular Biology, Indiana University School of Medicine-South Bend; Harper Cancer Research Institute, Notre Dame, IN; Department of Chemistry and Biochemistry, University of Notre Dame, Notre Dame, IN, United States

[9]Medical Sciences Program, Indiana University School of Medicine, Indiana University, Bloomington, IN, United States; Department of Cellular and Integrative Physiology, Indiana University School of Medicine, Indianapolis, IN, United States

Abstract

Objective—Genomic studies of ovarian cancer (OC) cell lines frequently used in research revealed that these cells do not fully represent high-grade serous ovarian cancer (HGSOC), the most common OC histologic type. However, OC lines that appear to genomically resemble HGSOC have not been extensively used and their growth characteristics in murine xenografts are essentially unknown.

*Co-corresponding authors

Methods—To better understand growth patterns and characteristics of HGSOC cell lines *in vivo*, CAOV3, COV362, KURAMOCHI, NIH-OVCAR3, OVCAR4, OVCAR5, OVCAR8, OVSAHO, OVKATE, SNU119, UWB1.289 cells were assessed for tumor formation in nude mice. Cells were injected intraperitoneally (i.p.) or subcutaneously (s.c.) in female athymic nude mice and allowed to grow (maximum of 90 days) and tumor formation was analyzed. All tumors were sectioned and assessed using H&E staining and immunohistochemistry for p53, PAX8 and WT1 expression.

Results—Six lines (OVCAR3, OVCAR4, OVCAR5, OVCAR8, CAOV3, and OVSAHO) formed i.p xenografts with HGSOC histology. OVKATE and COV362 formed s.c. tumors only. Rapid tumor formation was observed for OVCAR3, OVCAR5 and OVCAR8, but only OVCAR8 reliably formed ascites. Tumors derived from OVCAR3, OVCAR4, and OVKATE displayed papillary features. Of the 11 lines examined, three (Kuramochi, SNU119 and UWB1.289) were non-tumorigenic.

Conclusions—Our findings help further define which HGSOC cell models reliably generate tumors and/or ascites, critical information for preclinical drug development, validating *in vitro* findings, imaging and prevention studies by the OC research community.

Keywords

high grade serous ovarian cancer; xenograft; Pax8; mouse model

Introduction

Ovarian cancer (OC) is the fifth leading cause of cancer-related deaths among women in the US and the most lethal gynecologic malignancy[1]. The five-year survival rate has remained close to 25%, and all women are currently treated with the same approach consisting of surgical debulking followed by chemotherapy composed of paclitaxel and carboplatin[2]. Diagnosis of OC usually occurs after metastasis at stage II–IV, and this contributes to the poor survival [3]. Targeted therapies and better strategies for early detection would increase survival, but adequate model systems to study the disease remain a major challenge facing the gynecologic oncology research field [4, 5].

Ovarian cancer is a heterogeneous disease that includes at least five histotypes: clear cell, endometrioid, mucinous, low-grade serous, and high-grade serous tumors [6, 7]. Heterogeneity may be a result of the cell of origin that gives rise to different forms of the disease and reflects distinct molecular alterations associated with each histotype[8–10]. High-grade serous ovarian cancer (HGSOC), the most common and deadly form of the disease, is considered the “prototype” of epithelial OC, and the recent Cancer Genome Atlas Network analysis defined the landscape of deregulated pathways characterizing HGSOC[11]. Specifically, these tumors are classified based upon mutation of p53, BRCA1/2 mutation, somatic loss, or methylation, and a variety of protein markers including PAX8 and WT1. In addition, copy number variation is a hallmark of HGSOC and less commonly found in endometrioid, clear cell, and mucinous histotypes [12]. Recent genetic signatures from primary human tumors further divided HGSOC into four molecular groups, namely immunoreactive, proliferative, differentiated, and mesenchymal [13]. While these categories are well established in primary and recurrent HGSOC tumors, the ability to

correlate genomic and molecular features with useful laboratory model systems is critical for the future development of new therapies, prevention strategies, and imaging studies [14].

Recent publications have characterized an expanded panel of OC cell lines at the genomic level, in 2-dimesional-cell culture (on plastic), and in regards to their *in vitro* response to chemotherapeutic drugs [15–17]. These reports further suggested that OC cell lines commonly used in the past (e.g. SKOV3, A2780) do not represent a good approximation of the HGSOC genotype and that a panel of recently described cell lines more closely resemble human serous tumor. However, several of the newly proposed models for HGSOC have never been characterized for the ability to form tumors in immune deficient mice, which is critical to study mechanisms of disease or therapeutic interventions *in vivo*. The goal of this study was to determine the tumorigenic ability of newly described HGSOC cell lines and the histologic characteristics of the xenografts derived from these cells.

Materials and Methods

Cell culture

All reagents were obtained from Life Technologies (Carlsbad, CA) unless otherwise indicated. OVCAR4 was obtained through Material Transfer Agreement (MTA) from the National Cancer Institute for the transfer of cell lines from the Division of Cancer Treatment and Diagnosis Tumor Repository. The DCTD Tumor Repository has maintained, since the early 1960's, a low temperature repository of transplantable tumor and tumor cell lines from various species. OVCAR4 were maintained in RPMI supplemented with 10% fetal bovine serum (FBS), 2mM L-glutamine, and 100U/ml penicillin/streptomycin. Kuramochi, OVSAHO, and OVKATE were obtained through MTA from the Japanese Collection of Research Bioresources Cell Bank (JCRB). The JCRB cells were cultured in RPMI 1640 medium with 10% FBS. NIH:OVCAR3, CAOV3 and UWB1.289 cells were purchased from ATCC (1/2014). NIH:OVCAR3 cells were maintained In RPMI-1640 Media supplemented with 20% FBS, 0.01mg/ml insulin and 50 U/mL penicillin, and 50μg/mL streptomycin. CAOV3 cells were grown in Dulbecco's Modified Eagles Medium containing 10% FBS and 50 U/mL penicillin, and 50 μg/mL streptomycin. OVCAR5 cells were obtained from the Developmental Therapeutics Program at National Cancer Institute and cultured in DMEM, 10%FBS, 1% PSG, and 0.1mM MEM Non-essential amino acids. OVCAR8 cells were obtained from ATCC and cultured in DMEM with 10% FBS. COV362 were from Adam Karpf, Eppley Institute for Research in Cancer and Allied Diseases, University of Nebraska Medical Center and grown in DMEM with L-glutamine (300mg/L) and 10% heat inactivated fetal bovine serum. SNU-119 were sourced from the Korean Cell Line Bank (also obtained from Dr. Karpf) and grown in RPMI1640 with L-glutamine (300mg/L), 25mM HEPES and 25mM NaHCO3, 90%; heat inactivated fetal bovine serum (FBS), 10%. UWB1.289 cells were cultured in media composed of 1:1 RPMI-1640 and Mammary Epithelial Growth Medium (MEGM, Lonza #CC-3150) supplemented by 3% FBS. Information regarding mycoplasma testing, in vitro doubling times, and STR validation is in Supplemental Table 1.

Study approval

All animals were treated in accordance with the NIH guidelines for Laboratory Animals and established Institutional Animal Use and Care protocols at the University of Illinois at Chicago, Indiana University School of Medicine, Indiana University, Bloomington, and University of Notre Dame.

Xenografting

6–7 weeks old female athymic (nude) mice were acquired from (Harlan Teklad, Indianapolis, IN) and xenografted with human OC cells 1×10^6 cells subcutaneously (s.c) and 5×10^6 cells intraperitoneally (i.p.) in sterile PBS. Animal body weight and s.c. tumor growth (via caliper measurement) were tracked weekly and animals sacrificed when tumor burden was evident or general health was determined to be moribund. If no tumor formation was evident, animals were sacrificed after 90 days of tumor implantation.

Tissue collection and analysis

At the time of sacrifice, s.c. and i.p. tumors were dissected and weighed, and evidence of i.p. disease was noted by photography and charted based on organ of dissemination. Tissues were fixed in 4% paraformaldehyde before dehydration in ethanol and xylene prior to paraffin embedding. Immunohistochemistry and hematoxylin and eosin (H&E) staining was performed as previously described [18]. Briefly, tissues were sectioned and rehydrated in a gradient of ethanol prior to antigen retrieval and peroxidase block. Sections were incubated in primary antibody overnight at 4°C before detection via biotinylated secondary antibody (1:200, Vector Laboratories (Burlingame, CA) and ABC peroxidase (Vector Laboratories). Targets were visualized via 3,3'-diaminobenzidine (DAB, Vector Laboratories) and counterstained with hematoxylin. The following antibodies were used in the study: p53 (Santa Cruz Biotechnology sc-6243 dilution 1:50), Pax8 (Proteintech 10336-1-AP dilution 1:150), and WT1 (Abcam ab89901 dilution 1:50).

Results

To assess which HGSOC cell lines recapitulate OC clinical features *in vivo*, xenograft assays and pathologic characterization of resulting tumors were performed. Kuramochi, OVSAHO, SNU118, COV362, and OVCAR4 were the top five most likely to be high-grade serous ovarian cancer according to the genomic data analysis published by Domcke et al. [17]. The same report identified CAOV3, OVCAR3, and OVCAR8 as possible representatives of high-grade serous cancer. Additionally, CAOV3, Kuramochi, OVCAR3, OVCAR4, OVCAR5, and OVCAR8 were identified as high grade serous by Anglesio et al[15]. UWB1.289 was chosen because it is BRCA-null[19]. Eleven OC cell lines were injected i.p. and/or s.c. into female nu/nu mice and tumor formation was assessed after observation (up to 90 days). Six of the cell lines (OVCAR3, OVCAR4, OVCAR5, OVCAR8, CAOV3, and OVSAHO) formed i.p xenografts (Figure 1, Table 1) and considered tumorigenic. OVKATE and COV362 only formed s.c. tumors after 90 days and 77 days respectively with no evidence of tumor formation in the i.p. grafted mice. No tumor formation (either i.p. or s.c) was observed for Kuramochi, UWB1.289, and SNU119 after 90 days of observation, and these three OC lines were considered to be non-tumorigenic. The

data in Table 1 summarizes the average survival, number of tumors per mouse, and p53 mutational status for the cell lines evaluated[19–21].

As shown in Figure 1, the OVCAR 3 cell line formed the largest ($P < 0.05$) s.c. tumors by mass (400–970 mg by 36 days). OVCAR8 formed the largest i.p. tumors (1004–1509 mg by 27 days). The most rapid s.c. tumor formation was observed for OVCAR5 (26 days), OVCAR8 (27 days) and OVCAR3 (36 days), but s.c. tumor formation for the other cell lines tested took longer than 2 months (see Suppl. Fig. S1 for s.c. growth rate for tumors derived from OVCAR4, OVKATE and COV362 cells). For i.p. injections, 100% tumor take was seen for OVCAR3, OVCAR4, OVCAR5, OVCAR8, and CAOV3 cell lines, but only 80% for OVSAHO cells. The macroscopic appearance and distribution of i.p. tumors formed is shown in Figure 2.

The location of metastasis in the peritoneal space after i.p. injection was also examined. Disseminated tumorigenic cells were observed on peritoneal surfaces, the gastrointestinal tract, particularly the small bowel, and the omentum (Table 2), all typical sites of metastasis encountered in women with advanced stage HGSOC[5]. OVCAR3 tumors were the most widely metastatic, but interestingly malignant ascites formation was not recorded and gross metastases to the diaphragm were uncommon, despite the high tumorigenic potential of this OC line. For the models that formed i.p. disease, tumors in the GI tract were observed for all six cell lines, with the liver and reproductive tissues representing the other most common tumor sites. Only OVCAR8 consistently formed ascites fluid when grafted i.p. (within 90 days).

The microscopic appearance of OVAR3, OVCAR4, OVCAR5, OVCAR8, CAOV3, and OVSAHO derived xenografts was consistent with HGSOC histology (Figure 3). OVKATE and COV362 were also consistent in HGSOC histology, but as s.c. tumors only (neither line formed tumors i.p.). Strong nuclear staining for PAX8 and WT1, characteristic of HGSOC, was observed in OVCAR3, OVCAR4, CAOV3, OVCAR8, OVSAHO and OVKATE xenografts. Patchy and fainter PAX8 and WT1 nuclear staining was seen in OVCAR5 tumors (Figure 3 and Table 3). Strong nuclear p53 staining was observed in OVCAR3, OVCAR4, and OVKATE tumors, and faint p53 staining characterized OVSAHO, CAOV3, and OVCAR8 xenografts. Interestingly, OVCAR5 tumors were p53 negative (Figure 3), and tumorigenesis was also the most rapid for this line (Table 1). The published p53 mutation present in each cellular model is reported in Table 1. COV362 s.c. tumors only stained positively for Pax8 and not for WT1 or p53.

Discussion

Validation and comprehensive characterization of genetically and phenotypically defined human cell models are essential for the success of biomedical research to treat and prevent ovarian carcinoma. The cellular models most commonly used in the literature, such as SKOV3 and A2780, have been questioned as being valid models of the most deadly and common OC histotype, high grade serous carcinoma[15, 17]. While a few very recent publications have provided invaluable characterization of the mutational and growth characteristics of more representative cellular models of HGSOC, most of these have not

been studied in terms of their growth as a xenograft[15–17], and equally importantly the tumorigenic ability of these lines as xenografts in nude mice is unknown and thus their true potential for studying human HGSOC is uncertain.

The current study is the first to compile and directly compare the *in vivo* xenograft characteristics of several HGSOC cellular models. Intriguingly, of the top five models suggested for use based on genomic sequencing, including Kuramochi, OVSAHO, SNU119, COV362, and OVCAR4, only two formed intraperitoneal tumors in athymic nude mice within 90 days. Furthermore, we show that of the cell models that *in vivo* most resemble the papillary characteristic of high-grade serous cancer (OVCAR3, OVCAR4, and OVKATE), only OVKATE formed s.c. xenograft tumors within 90 days, although it is possible that xenografting a higher number of cells for a longer period might result in i.p. disease. Of the 11 cell models examined in this study, only OVCAR8 reliably demonstrated ascites formation within 90 days, and SNU119, Kuramochi, and UWB1.298 all failed to form tumors. Overall, we demonstrate the utility of several cellular models for *in vivo* xenografting and illustrate their unique peritoneal dissemination pattern.

In vivo growth characteristics of HGSOC cell models may help dictate their application. For example, OVCAR3, OVCAR5, and OVCAR8, the most aggressive lines based on their rapid growth *in vivo*, may be useful to reduce the length and cost of xenograft studies. However, because OVCAR5 and OVCAR8 i.p. tumor growth is widely disseminated, it may be a challenge to quantitate initial tumor burden as well as changes in tumor growth in response to therapy. Take rates were remarkably consistent between the cell models that produced tumors, suggesting that if grafted, these models are reliable. OVSAHO and OVKATE were both very slow growing *in vivo* and *in vitro*, and it seems reasonable to suggest that they would both form i.p. disease with more cells or more time. OVCAR3 and OVCAR8 formed the largest tumor masses and these lines may be extremely useful in conjunction with *in vivo* optical imaging technologies or drug accumulation and biodistribution studies with nanocarriers. For the cells that formed tumors, there was a remarkable divergence in organs colonized, although the organs were similar to those seen in human disease. All cell models colonized the GI tract and liver and the second most common site of tumor formation was the reproductive tract, suggesting that these models may be appropriate to study interactions between tumor cells and the microenvironment, in general as well as at specific sites *in vivo*.

In this initial analysis, there was no apparent correlation between the mutational spectrum of the cell lines and *in vivo* growth characteristics. All of the models in this study have p53 mutations except for OVCAR5, which is p53 null. Otherwise the mutational spectrum for these lines is dramatically different, and each could therefore be a model for a specific target, such as BRCA1 (for COV362 as a s.c. model), c-myc (COV362 as a s.c. model), cyclin E (OVCAR3), mutation in ERBB2 (OVCAR8) or loss of Rb (OVSAHO)[17]. Interestingly, previous reports based on *in vitro* immunocytochemistry studies performed on the cell lines found CAOV3 and OVCAR4 to be negative for p53 and WT1. In contrast, our *in vivo* study found that these markers are expressed in tumors from both of these cell lines [16]. OVCAR5 and OVCAR3 were identical at the cellular and tumor level for p53 and WT1 expression. OVCAR8 expressed WT1 mostly in the nucleolar compartment, which has

previously been described in mucinous tumors [22]. Only three of the models tested here *in vivo* (COV362, OVCAR3, and CAOV3) were also screened for chemotherapy sensitivity *in vitro*[16]. All three models appeared to be relatively sensitive to chemotherapy and also had almost exactly the same doubling time *in vitro*, between 51–56 hours [16], yet *in vivo* OVCAR3 was much more aggressive (Figure 1). In summary, the development of more reliable and authenticated models of HGSOC has been dramatically improved by recent reports characterizing their genomes, behavior *in vitro*, and sensitivity to drugs. This report adds to the growing information and helps to define which HGSOC models reliably generate tumors and/or ascites, essential information for their use in drug discovery, imaging, and prevention studies.

Supplementary Material

Refer to Web version on PubMed Central for supplementary material.

Acknowledgements

The authors thank Sue Childress and Jay Pilrose for technical assistance. This work was supported in part by grants RSG-12-230-01-TBG from the American Cancer Society Illinois Division and DOD OCRP OC130046 (JEB), the Ovarian Cancer Research Foundation Liz Tilberis Scholar Award (MVB, JEB, and KCD), NIH/NCI grants CA109545 (MSS), CA086984 (MSS), V Foundation and NIH/NCI CA182832 (DM and KPN), and NSF DGE1313583 (EL). We would like to acknowledge the generous donation from Adam Karpf of the COV362 cell line.

References

1. Siegel R, Ma J, Zou Z, Jemal A. Cancer statistics, 2014. CA Cancer J Clin. 2014; 64:9–29. [PubMed: 24399786]
2. Schmid BC, Oehler MK. New perspectives in ovarian cancer treatment. Maturitas. 2014; 77:128–136. [PubMed: 24380827]
3. Vaughan S, Coward JI, Bast RC Jr, Berchuck A, Berek JS, Brenton JD, et al. Rethinking ovarian cancer: recommendations for improving outcomes. Nat Rev Cancer. 2011; 11:719–725. [PubMed: 21941283]
4. Banerjee S, Kaye S. The role of targeted therapy in ovarian cancer. Eur J Cancer. 2011; 47(Suppl 3):S116–S130. [PubMed: 21943965]
5. Banerjee S, Kaye SB. New strategies in the treatment of ovarian cancer: current clinical perspectives and future potential. Clin Cancer Res. 2013; 19:961–968. [PubMed: 23307860]
6. Auersperg N. The origin of ovarian carcinomas: a unifying hypothesis. Int J Gynecol Pathol. 2011; 30:12–21. [PubMed: 21131839]
7. Auersperg N, Edelson MI, Mok SC, Johnson SW, Hamilton TC. The biology of ovarian cancer. Semin Oncol. 1998; 25:281–304. [PubMed: 9633841]
8. Auersperg N. The origin of ovarian cancers - hypotheses and controversies. Front Biosci (Schol Ed). 2013; 5:709–719. [PubMed: 23277080]
9. Crum CP, Herfs M, Ning G, Bijron JG, Howitt BE, Jimenez CA, et al. Through the glass darkly: intraepithelial neoplasia, top-down differentiation, and the road to ovarian cancer. J Pathol. 2013; 231:402–412. [PubMed: 24030860]
10. Dubeau L, Drapkin R. Coming into focus: the nonovarian origins of ovarian cancer. Ann Oncol. 2013; 24(Suppl 8):viii28–viii35. [PubMed: 24131966]
11. Integrated genomic analyses of ovarian carcinoma. Nature. 2011; 474:609–615. [PubMed: 21720365]
12. Huang RY, Chen GB, Matsumura N, Lai HC, Mori S, Li J, et al. Histotype-specific copy-number alterations in ovarian cancer. BMC Med Genomics. 2012; 5:47. [PubMed: 23078675]

13. Verhaak RG, Tamayo P, Yang JY, Hubbard D, Zhang H, Creighton CJ, et al. Prognostically relevant gene signatures of high-grade serous ovarian carcinoma. J Clin Invest. 2013; 123:517–525. [PubMed: 23257362]
14. Lengyel E, Burdette JE, Kenny HA, Matei D, Pilrose J, Haluska P, et al. Epithelial ovarian cancer experimental models. Oncogene. 2014; 33:3619–3633. [PubMed: 23934194]
15. Anglesio MS, Wiegand KC, Melnyk N, Chow C, Salamanca C, Prentice LM, et al. Type-specific cell line models for type-specific ovarian cancer research. PLoS One. 2013; 8:e72162. [PubMed: 24023729]
16. Beaufort CM, Helmijr JC, Piskorz AM, Hoogstraat M, Ruigrok-Ritstier K, Besselink N, et al. Ovarian cancer cell line panel (OCCP): clinical importance of in vitro morphological subtypes. PLoS One. 2014; 9:e103988. [PubMed: 25230021]
17. Domcke S, Sinha R, Levine DA, Sander C, Schultz N. Evaluating cell lines as tumour models by comparison of genomic profiles. Nature communications. 2013; 4:2126.
18. King SM, Hilliard TS, Wu LY, Jaffe RC, Fazleabas AT, Burdette JE. The impact of ovulation on fallopian tube epithelial cells: evaluating three hypotheses connecting ovulation and serous ovarian cancer. Endocr Relat Cancer. 2011; 18:627–642. [PubMed: 21813729]
19. DelloRusso C, Welcsh PL, Wang W, Garcia RL, King MC, Swisher EM. Functional characterization of a novel BRCA1-null ovarian cancer cell line in response to ionizing radiation. Mol Cancer Res. 2007; 5:35–45. [PubMed: 17259345]
20. Barretina J, Caponigro G, Stransky N, Venkatesan K, Margolin AA, Kim S, et al. The Cancer Cell Line Encyclopedia enables predictive modelling of anticancer drug sensitivity. Nature. 2012; 483:603–607. [PubMed: 22460905]
21. Bykov VJ, Issaeva N, Selivanova G, Wiman KG. Mutant p53-dependent growth suppression distinguishes PRIMA-1 from known anticancer drugs: a statistical analysis of information in the National Cancer Institute database. Carcinogenesis. 2002; 23:2011–2018. [PubMed: 12507923]
22. Shan W, Mercado-Uribe I, Zhang J, Rosen D, Zhang S, Wei J, et al. Mucinous adenocarcinoma developed from human fallopian tube epithelial cells through defined genetic modifications. Cell Cycle. 2012; 11:2107–2113. [PubMed: 22592533]

Highlights

- Eleven human cell models of high-grade serous ovarian cancer were tested in vivo tumor formation.
- OVCAR3, OVCAR5, and OVCAR8 were the most aggressive and OVCAR8 formed ascites.
- All six models formed peritoneal disease mimicking human cancer expressing p53, Pax8, and WT1.

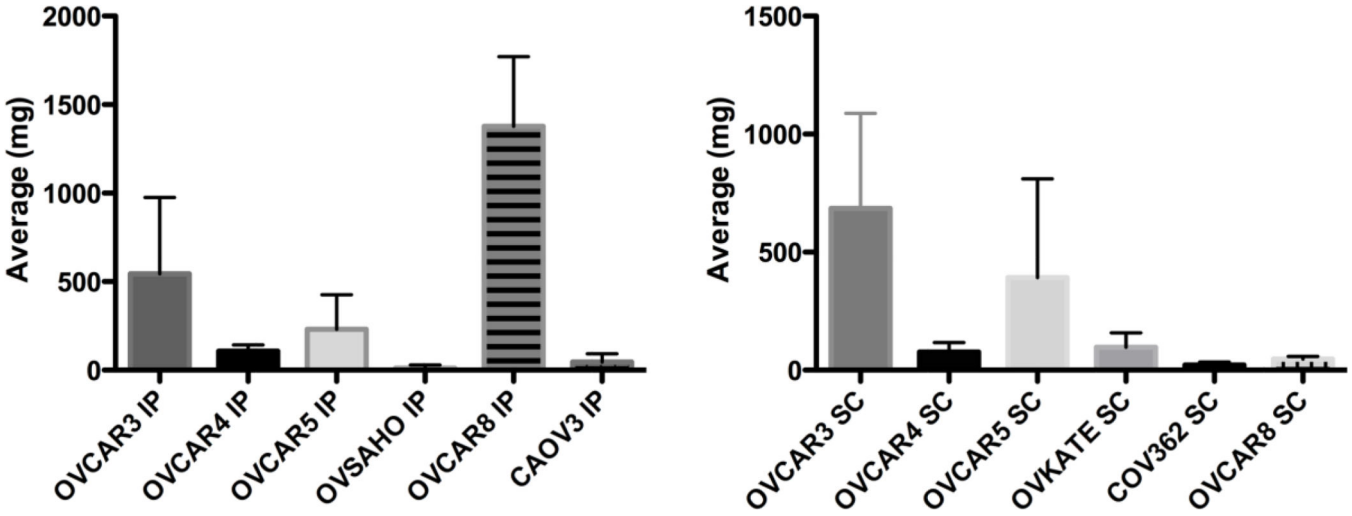

Figure 1.

Average tumor weight. Animals were sacrificed at 90 days unless tumor burden required euthanasia at an earlier time point (summarized in Table 1). Most cell models formed both intraperitoneal (i.p.; left) and subcutaneous (s.c.; right) tumors, but OVSAHO only formed IP and OVKATE and COV362 only formed SC.

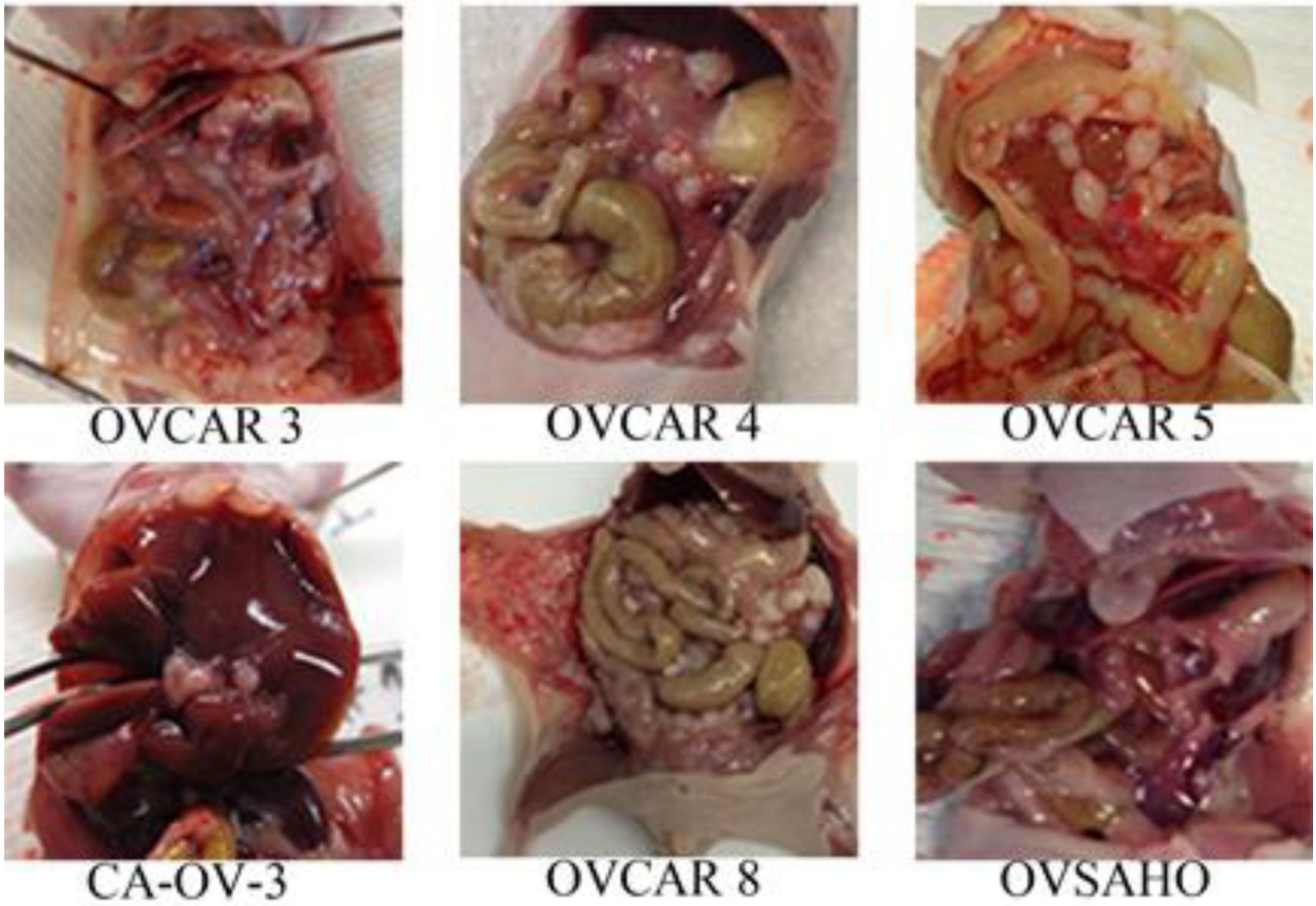

Figure 2.

Intraperitoneal (i.p.) dissemination of ovarian cancer cell lines in athymic nude mice. Cell models demonstrated unique sites of colonization (summarized in Table 2). Pictures are shown at time of dissection from a representative mouse with i.p. tumors

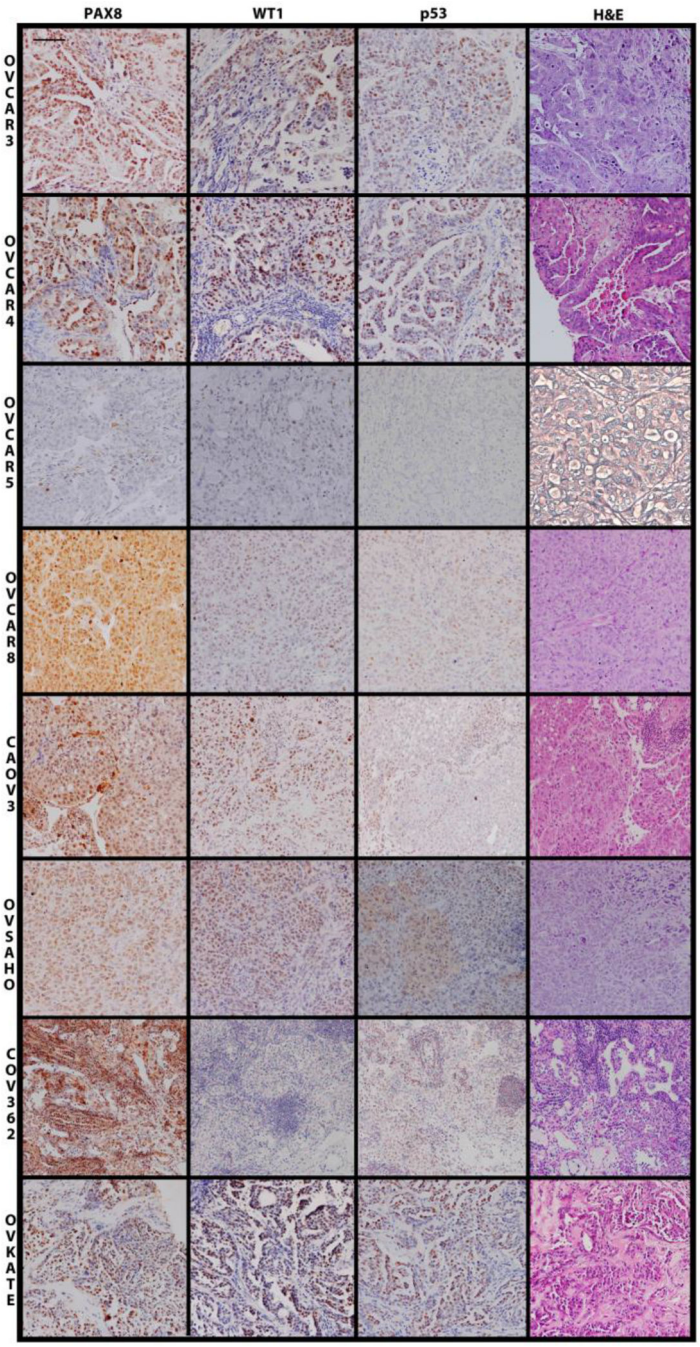

Figure 3.

Human ovarian cancer cell models form high-grade serous tumors based on histology and protein expression. Cell models that formed intraperitoneal tumors are shown except for OVKATE and COV362, which only grew subcutaneous tumors. Histology and immunohistochemical staining of PAX8, WT1, and p53 are shown for human cell models. Scale bars equal 50 microns.

Table 1

Tumor latency, number, take rate, and ascites formation.

	OVCAR3	OVCAR4	OVCAR5	OVCAR8	CAOV3	COV362	OVSAHO	OVKATE	Kuramochi	SNU119	UWB1.289 BRCA null
Days Until Sacrifice (IP)	64 days	90 days	26 days	44 days	90 days	90 days	90 days	90 days	90 days	90 days	90 days
Days Until Sacrifice (SC)	36 days	90 days	26 days	27 days	100 days	77 days	90 days	90 days	90 days	90 days	90 days
Average # of IP Tumors/mouse	10.7	11.2	161.4	207.4	8.8	0/8	1.4	0/5	0/5	0/8	0/5
Tumor Range (IP)	1 – 20	7 – 13	0 – 409	148 – 248	2 – 21	N/A	0 – 3	N/A	N/A	N/A	N/A
Tumor Take (IP)	6/6	5/5	4/5	5/5	6/6	0/8	4/5	0/5	0/5	0/8	0/5
Tumor Take (SC)	2/3	4/4	5/5	3/3	0/3	7/9	0/5	4/4	0/3	0/5	0/5
Ascites	1/6	0/5	0/5	4/5	0/6	0/8	0/5	0/5	0/5	0/5	0/5
TP53 status (base/mutation)	248[20] C→T	130[20] G→C	224[21] insertion/null	126[20] in frame deletion	136[20] G→A	220[20] T→C	342[20] G→A	282[20] G→A	281[20] C→A	151[20] G→A	625 Del AG[19]
BRCA1	-	-	-	-	-	1336-splice 871-frame shift	-	-	-	-	-
BRCA2	-	-	-	-	-	-	Del[17]	-	2318[20] C→T	-	-
MYC	-	-	-	-	-	Ampli[17]	-	-	Ampli[17]	Ampli[17]	-
KRAS	-	-	-	121[20] G→T	-	-	-	-	Ampli[17]	-	-
CCNE1	Ampli[17]	-	-	-	-	-	-	-	-	-	-
RB1	-	-	-	-	-	Ampli[17]	Ampli[17]	-	-	-	-

Table 2

Sites of HGSC peritoneal colonization

	OVCAR3	OVCAR4	OVCAR5	OVCAR8	CAOV3	OVSAHO
Reproductive Tract	1/6	2/5	2/5	5/5	2/6	0/5
G.I. Tract	4/6	4/5	4/5	5/5	3/6	3/5
Omentum	2/6	5/5	0/5	5/5	6/6	0/5
Peritoneal wall	0/6	0/5	0/5	5/5	1/6	0/5
Diaphragm	0/6	0/5	0/5	5/5	3/6	0/5
Pancreas	2/6	0/5	4/5	0/5	0/6	0/5
Kidney	2/6	0/5	0/5	0/5	0/6	0/5
Liver	1/6	2/5	2/5	5/5	5/6	1/5
Injection site	2/6	0/5	0/5	0/5	3/6	0/5

Table 3

Summary of immunohistochemistry

All results are from i.p. tumors except for OVKATE and COV362, which only formed s.c. tumors.

	OVCAR3	OVCAR4	OVCAR5	OVCAR8	CAOV3	COV362	OVSAHO	OVKATE
PAX8	+	+	−	+	+	+	+	+
WT1	+	+	−	nucleolar	+	−	+	+
p53	+	+	null	weak	+	−	+	+